Tuning pyrolysis temperature to improve the in-line steam reforming catalyst activity and stability

Enara Fernandez [a], Maria Cortazar [a], Laura Santamaria [a], Maite Artetxe [a], Maider Amutio [a], Gartzen Lopez [a,b,*], Javier Bilbao [a], Martin Olazar [a]

[a] Department of Chemical Engineering, University of the Basque Country UPV/EHU, P.O. Box 644, E48080 Bilbao, Spain
[b] IKERBASQUE, Basque Foundation for Science, Bilbao, Spain

ARTICLE INFO

ABSTRACT

This study analyzes the two-step process of biomass pyrolysis and in-line steam reforming for the production of H_2. In order to evaluate the effect of the volatile composition on the commercial Ni/Al_2O_3 catalyst performance and stability, biomass pyrolysis step was conducted at different temperatures (500–800 °C). The analysis of the deactivated catalysts has also allowed identifying the main bio-oil compounds responsible for catalyst decay (coke precursors). Pyrolysis temperature allows modifying the composition of the volatile stream that is subsequently reformed at 600 °C. An increase in pyrolysis temperature to 800 °C improves considerably the production of both H_2 and gaseous stream at the initial reaction stages, reaching values of 12.95 wt% and 2.23 Nm^3 kg^{-1}, respectively. Catalyst stability is also considerably improved when pyrolysis temperature is increased due to the lower bio-oil yield and its different composition at high temperatures. Coke was the main cause of catalyst deactivation. Besides, the nature of the coke deposited is influenced by the composition of the pyrolysis volatiles, with encapsulating coke being formed by the adsorption and subsequent condensation of all hydrocarbons (oxygenated and non-oxygenated ones) preferably at low temperatures, whereas filamentous coke is formed when the concentrations of CO and light hydrocarbons in the volatile stream are increased at 800 °C.

1. Introduction

The depletion of fossil fuels and the concern on climate change have increased in the last decades. Aiming to reduce fossil fuel dependence and CO_2 emissions, research on sustainable fuels has become essential, with hydrogen being a clean alternative to carbon containing fossil fuels for many applications (Ahmed et al., 2016; Wang et al., 2022; Meloni et al., 2022). Among different hydrogen production alternatives from renewable feedstocks, biomass conversion by thermochemical routes has attracted great attention (Arregi et al., 2018a; Dou et al., 2019; Kumar and Strezov, 2021; Okolie et al., 2022; Martino et al., 2021), with the most studied routes in the literature being: i) biomass steam gasification (Cao et al., 2020; Hayashi et al., 2006), and ii) catalytic bio-oil steam reforming (Kumar et al., 2017; Zhao et al., 2020; Lemonidou et al., 2013a). Although the catalytic steam reforming of bio-oil is a promising technology for hydrogen production, the direct strategy of biomass pyrolysis and in-line catalytic steam reforming has gained attention as an alternative route, as it avoids operational problems related to bio-oil handling, such as storage and vaporization (Arregi et al., 2018a; Lopez et al., 2022).

The performance and stability of the catalysts used in the steam reforming of bio-oil and other biomass derived oxygenates have been extensively discussed in literature (Setiabudi et al., 2020; Li et al., 2016; Cortazar et al., 2021a). Thus, Ni-based catalysts are considered efficient for the steam reforming of bio-oil due to their activity for breaking C-C and O-H bonds and moderate cost compared to noble metals (Chen et al., 2017). Nevertheless, Ni catalysts are prone to undergo deactivation due to coke deposition on the surface of Ni active sites and sintering of Ni particles (Li et al., 2020; Ochoa et al., 2020). With the aim of minimizing the deactivation of Ni reforming catalysts, numerous studies have focused on their optimization (Santamaria et al., 2021; Ashok and Kawi, 2021; Gao et al., 2021). On the one hand, alternative supports to the most used Al_2O_3 have been studied (mainly ZrO_2, TiO_2, CeO_2, MgO, SiO_2 (Huang et al., 2021; Santamaria et al., 2019; Men et al., 2007; Palma et al., 2018a) and diverse low-cost materials (Tang et al., 2021; Quan et al., 2020; Di Stasi et al., 2021) in order to provide the catalyst with

high specific surface area, adequate pore distribution, mechanical strength, thermal stability and acidity or basicity. On the other hand, alkali metals (Li, Na, K), alkaline-earth metals (Mg, Ca, Ba), rare earth oxides (La_2O_3, CeO_2) or transition metal oxides (ZrO_2, ZnO) have been incorporated into the catalyst as promoters (Alvarez et al., 2014; Lemonidou et al., 2013b; Santamaria et al., 2020a; Zhang et al., 2019) in order to improve its activity, selectivity and stability, as their incorporation enhances metal dispersion, reducibility, metal-support interaction and coke resistance.

Besides, many attempts have been carried out in the literature in order to attenuate Ni catalysts deactivation in the bio-oil steam reforming, such as those involving different reactor configurations (Kumar and Strezov, 2021). Among them, the fluidized bed reactor is considered the most appropriated for minimizing coke deposition (Adeniyi et al., 2019; Palma et al., 2018b), but fast catalyst deactivation by coke deposition is still its main drawback. Likewise, several authors proposed a two-step reaction system, in which a low cost material (conditioning catalyst) is located in a pre-reforming step in order to modify the composition of the volatile stream, and so attenuate the deactivation of the reforming catalyst (García-Gómez et al., 2021; Liu et al., 2019; Fernandez et al., 2021a). Remiro et al. (Remiro et al., 2013) also implemented a two-step reaction system made up of a thermal step for treating the raw bio-oil and a subsequent reforming one for hydrogen production, which allows a controlled carbonaceous solid deposition in the thermal step and so the attenuation of reforming catalyst deactivation.

The bio-oil obtained from biomass pyrolysis is a complex mixture of different oxygenated compounds with various functionalities, such as acids, ketones, alcohols, phenols, guiacols etc., and their reforming involves a complex reaction network (Remiro et al., 2013; Remón et al., 2015; Zhang et al., 2020a). Thus, in order to understand the relationship between reactivity, hydrogen production potential and coke formation from different oxygenates, several studies have approached the steam reforming of bio-oil model compounds (Li et al., 2020; González-Gil et al., 2015; Vagia and Lemonidou, 2010). However, their reforming behavior is different when they are alone or are part of the bio-oil, as interactions occur between them and other bio-oil components.

In order to progress towards the scaling up of the pyrolysis and in-line steam reforming, a rigorous evaluation of the role played by bio-oil composition on the catalysts performance is required. Therefore, this paper focuses on studying the influence of pyrolysis temperature on the composition of the volatiles and its impact on hydrogen production and catalyst stability in the subsequent reforming step. Accordingly, a conical spouted bed reactor (CSBR) was used for biomass fast pyrolysis and a fluidized bed reactor (FBR) for the reforming of the volatile stream. Furthermore, the knowledge acquired by modifying the composition of the stream entering the reforming stage allows determining the main bio-oil compounds responsible for the deactivation of the reforming catalyst. Thus, catalyst deactivation has been monitored and the coke deposited on the catalyst surface has been studied by means of temperature programmed oxidation (TPO) and transmission electron microscopy (TEM).

2. Experimental

2.1. Materials

Pinewood waste (pinus insignis) has been the biomass used in this study, which has been crushed and sieved to a particle size in the range from 1 to 2 mm. Table 1 shows the properties of the biomass, which have been determined by ultimate and proximate analysis in a LECO CHNS-932 elemental analyzer and TGA Q5000IR thermogravimetric analyzer, respectively. Furthermore, an isoperibolic bomb calorimeter (Parr 1356) has been used to determine the higher heating value (HHV).

In addition, a commercial Ni based catalyst (ReforMax®330 or G90-LDP) has been used in the steam reforming of biomass pyrolysis volatiles

Table 1

Pinewood sawdust characterization.

Ultimate analysis (wt%)[a]	
Carbon	49.33
Hydrogen	6.06
Nitrogen	0.04
Oxygen[b]	44.57
Proximate analysis (wt%)[c]	
Volatile matter	73.4
Fixed carbon	16.7
Ash	0.5
Moisture	9.4
Macromolecular composition (wt%)[d]	
Cellulose	35.7
Hemicelluloses	21.9
Lignin	33.1
HHV (MJ kg^{-1})	19.8

[a] on a dry ash free basis
[b] by difference
[c] on an air-dried basis
[d] determined in a previous study by thermogravimetric analysis (TGA) (Saldarriaga et al., 2015).

(specifically designed for CH_4 reforming). The catalyst was supplied by Süd Chemie in the form of perforated rings (19 ×16 mm), and was ground and sieved to a particle size in the 0.4–0.8 mm range. The chemical composition of the reforming catalyst is based on NiO (nominal content of 14 wt%), $CaAl_2O_4$ and Al_2O_3. The textural properties obtained by N_2 adsorption-desorption (Micromeritics ASAP 2010) revealed a mesoporous material with an average pore diameter of 122 Å and a low BET surface area (19 m^2 g^{-1}) (Erkiaga et al., 2015; Lopez et al., 2015).

Moreover, temperature programmed reduction (TPR) was conducted in a *Micromeritics AutoChem2920* to determine the catalyst reduction temperature, and the results are available in previous papers (Erkiaga et al., 2015; Lopez et al., 2015). They revealed two main peaks: i) one around 550 °C, which was ascribed to the reduction of NiO and ii) another one at 700 °C related to $NiAl_2O_4$ spinel phase. Therefore, prior to the pyrolysis and in-line steam reforming runs, the reforming catalyst has been reduced in-situ by feeding 10 vol% H_2/N_2 stream at 700 °C for 4 h.

2.2. Experimental equipment

The scheme of the bench scale plant used for biomass pyrolysis-reforming is shown in Fig. 1. The plant is equipped with a conical spouted bed reactor (CSBR) for biomass pyrolysis and a fluidized bed reactor (FBR) for the reforming of the volatiles formed in the first step.

The design of the CSBR allows a vigorous solid movement and ensures flash pyrolysis conditions due to the high heat transfer rates and low gas residence times. Moreover, previous studies demonstrated the good performance of this reactor configuration for different feeds, such as biomass (Alvarez et al., 2019a; Amutio et al., 2015, 2013), plastics (Artetxe et al., 2015) and tyres (Alvarez et al., 2017).

Based on previous hydrodynamic studies, the following optimum dimensions were established for the CSBR: height of the conical section, 73 mm; diameter of the bed bottom, 12.5 mm; and diameter of the gas inlet, 7.6 mm. Moreover, the reactor has a gas preheating section, which consists of a stainless steel cylindrical shell filled with stainless steel pipes in order to increase the surface area for heat transfer, and so ensure the gases reach the bed at the desired temperature. Both the CSBR and the preheater are located inside a radiant ceramic fiber oven of 1250 W. A lateral outlet pipe is placed above the bed surface, which ensures the continuous removal of the char particles.

The volatiles (non-condensable gases and bio-oil oxygenated compounds) produced in the pyrolysis step are reformed in a fluidized bed reactor (FBR), whose dimensions are as follows: 38.1 mm internal diameter and 440 mm long. This reactor is located inside an oven
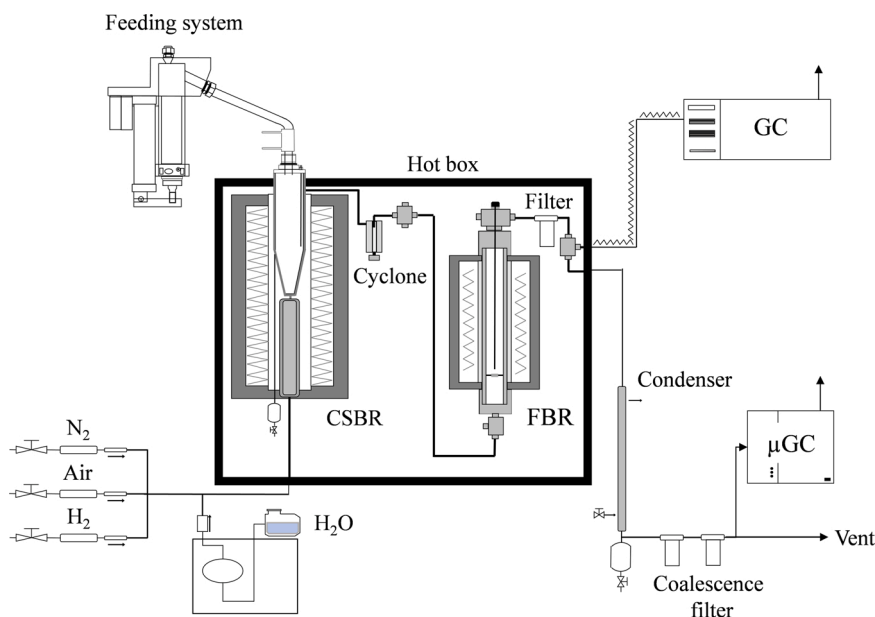
Fig. 1. Scheme of the laboratory scale plant.

(550 W) controlled by a thermocouple inserted in the catalytic bed. This reactor configuration eases the operation under isothermal conditions and minimizes plugging problems by coke deposition (Fernandez et al., 2021b).

Furthermore, the plant is provided with a cyclone, which removes the fine char particles entrained from the CSBR prior to feeding the volatiles into the reforming reactor, whereas the volatile stream leaving the FBR circulates through a sintered steel filter (5 μm), wherein elutriated catalyst fines are retained. In order to avoid the condensation of steam or pyrolysis products in the connection elements, the reaction equipment is located inside a forced convection oven, which maintains the box temperature at 300 °C.

The reaction equipment is provided with different devices, which allow continuous feeding of biomass, water and gases (N_2, air, H_2). The biomass feeding system is made up of a cylindrical vessel wherein the biomass is located on a piston raised by a shaft. The biomass overflows at the top of the cylinder and is fed into the CSBR through a pipe cooled with tap water. Moreover, a small N_2 flow rate is introduced into the feeder with the aim of avoiding the condensation of pyrolysis vapors and backflow of steam into the feeding vessel.

The water required in the reforming step is supplied by a Gilson 307 pump, which is vaporized in a heating cartridge located inside the hot box prior to entering the reactor. In addition, different gases (N_2, air, H_2) may be fed into the pyrolysis reactor. Nitrogen was used as fluidizing agent during the heating process and, once the reaction temperature was reached, the fluidizing agent was changed from N_2 to steam. Biomass feeding started when suitable spouting and fluidization were attained in the reactors. In the case of H_2, it was used for in-situ reduction of the Ni catalyst prior to the reforming reaction.

To ensure the collection of non-reacted steam and bio-oil derived compounds prior to the microGC analysis, the pilot plant is provided with a condensation system made up of a condenser cooled with tap water and coalescence filter.

2.3. Experimental conditions

Pyrolysis step was carried out at 500, 600, 700 and 800 °C. Based on previous hydrodynamics studies, a CSBR containing 50 g of silica sand with a particle size in the 0.3–0.355 mm range was used. Moreover, in order to ensure suitable fluidization regime in both the CSBR and the FBR, the water flow rate used in all the runs was 3 mL min^{-1}, which

corresponds to a steam flow rate of 3.73 NL min^{-1}.

In the reforming step, the operating conditions were established based on the optimum ones reported in previous biomass pyrolysis-reforming runs (Arregi et al., 2016). Thus, the reforming step was conducted at 600 °C in all the runs, as an increase in temperature to 700 °C barely improves process performance (Arregi et al., 2018b) and may lead to Ni sintering (Santamaria et al., 2021; Moulijn et al., 2001). The bed in the FBR was made up of a mixture of reforming catalyst and inert sand, with the total mass being 25 g. The particle size of the catalyst was in the 0.4–0.8 mm range and that of the inert silica sand in the 0.3–0.355 mm range. The steam/biomass (S/B) ratio was set at a value of 4, with a continuous biomass feeding rate of 0.75 g min^{-1} and a space time of 15 g_{cat} min $g_{volatiles}^{-1}$.

2.4. Product analysis

The biomass pyrolysis products at different temperatures were determined based on specific runs prior to those of pyrolysis-reforming. The volatile stream is analyzed on-line in a gas chromatograph (GC Agilent 6890) provided with a HP-Pona column (50 m length, 0.2 mm diameter and 0.5 μm film thickness) and a flame ionization detector (FID). For the products quantification, this sample is previously diluted in an inert gas and mixed with 0.075 mL min^{-1} of an external standard (cyclohexane) and injected into the GC by means of a line thermostated at 280 °C. FID response factors were used in the GC for the quantification of the main oxygenated compounds in the biomass pyrolysis volatile stream, which were determined in previous studies by using standard mixtures (Alvarez et al., 2017). A gas chromatograph-mass spectrometer (GC-MS Shimadzu QP-2010S) was used to identify the bio-oil compounds. A micro-gas chromatograph (Varian 4900) was used to analyze the permanent gases (H_2, CO_2, CO, CH_4 and C_2-C_4 hydrocarbons). The char fraction was collected through a lateral outlet, weighed, and analyzed by N_2 adsorption-desorption in a Micromeritics ASAP 2010. The water yield in the bio-oil sample was determined based on H mass balances by considering the H contained in the biomass (including moisture) and pyrolysis products. C, H and O mass balance closures were above 95% in all the runs, and they were repeated at least 3 times under the same experimental conditions in order to ensure reproducibility.

The analysis of the products obtained in all pyrolysis-reforming experimental runs was carried out by means of on-line chromatographic techniques. Accordingly, the volatiles leaving the reforming

reactor were analyzed by gas chromatography (GC Agilent 6890). This sample, previously diluted with an inert gas, was injected into the GC by means of a line thermostated at 280 °C. The permanent gases (H_2, CO_2, CO, CH_4 and C_2-C_4 hydrocarbons) were analyzed in a micro-chromatograph (GC Varian 4900) once the reforming outlet stream was condensed (cooled with tap water) and filtered (coalescence element).

Both the GC and the microGC analyses were carried out after several minutes operation to ensure steady state conditions. Furthermore, the analyses were repeated at least 3 times under the same conditions to guarantee reproducibility of the results.

The deactivated catalysts were characterized at the end of each continuous pyrolysis-reforming experiments by Temperature Programmed Oxidation (TPO) in a *Thermobalance (TGA Q5000 TA Instruments)*. The TPO was performed with a heating rate of 5 °C min^{-1} from 100 to 800 °C under 50 mL min^{-1} air stream. The total amount of coke was determined based on the mass gain in the oxidation of the metallic phase, with the same procedure being applied to the fresh reduced-catalyst. Moreover, the morphology of the coke was assessed by Transmission Electron Microscopy (TEM) in a *Philips SuperTwin CM200* microscope.

2.5. Reaction indices

In order to evaluate the influence of the pyrolysis volatiles composition on the commercial Ni/Al_2O_3 (G90-LDP) reforming catalyst performance, reforming conversion and individual product yields have been monitored.

Consequently, the volatile conversion in the reforming reactor is defined as the ratio between the C moles in the gaseous product (C_{gas}) and C moles in the feed of the reforming step ($C_{volatiles}$):

$$X = \frac{C_{gas}}{C_{volatiles}} \cdot 100 \tag{1}$$

It should be noted that the C amount contained in the char produced in the pyrolysis step is not considered in Eq. (1).

Likewise, the yield of each carbon containing gaseous product is calculated as the ratio between the molar flow rate of compound i (F_i) and the molar flow rate of the volatile stream ($F_{volatiles}$):

$$Y_i = \frac{F_i}{F_{volatiles}} \cdot 100 \tag{2}$$

The hydrogen yield was defined based on the maximum allowable by stoichiometry:

$$Y_{H_2} = \frac{F_{H_2}}{F_{H_2}^0} \cdot 100 \tag{3}$$

where F_{H2} is the H_2 molar flow rate and F_{H2}^0 the maximum allowable by the following stoichiometry:

$$C_nH_mO_k + (2n-k)H_2O \rightarrow nCO_2 + (2n + m/2-k)H_2 \tag{4}$$
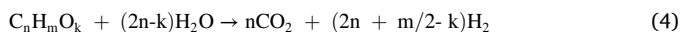
Finally, H_2 production is defined by mass unit of the biomass in the feed:

$$Prod._{H_2} = \frac{m_{H_2}}{m_{biomass}^0} \cdot 100 \tag{5}$$

where m_{H2} and $m_{biomass}^0$ are the mass flow rates of the H_2 produced and biomass fed into the process, respectively.

3. Results

3.1. Effect of temperature on the biomass pyrolysis stream (first step)

Biomass pyrolysis was conducted at different temperatures, i.e., 500, 600, 700 and 800 °C, using steam as fluidizing agent. The products

obtained in the pyrolysis step were grouped into three different fractions: i) gaseous fraction, composed of CO_2, CO, H_2 and small amounts of C_1-C_4 hydrocarbons, ii) condensable fraction, composed of a mixture of oxygenated compounds and water, and iii) solid fraction or char, which is the biomass fraction that cannot be volatilized under the selected operating conditions. Table 2 sets out the yields of the pyrolysis product fractions obtained at the different pyrolysis temperatures tested in the CSBR, whereas Table 3 shows the individual yields of bio-oil compounds.

As observed, temperature has a considerable effect on the yields of product fractions (Table 2), with the gas fraction yield increasing from 7.30 wt% at 500 °C to 63.92 wt% at 800 °C. Therefore, a significant decrease in the yields of bio-oil and char is observed, i.e., from 75.36 wt % and 17.34 wt% at 500 °C to 27.22 wt% and 8.86 wt% at 800 °C, respectively. It is well-known that an increase in pyrolysis temperature enhances not only the devolatilization of biomass components, but also secondary cracking reactions at high temperatures, favoring the formation of the gas fraction in detriment of the bio-oil fraction (Kan et al., 2020; Akhtar and Saidina Amin, 2012).

Besides, the role played by steam in the reaction mechanism changes depending on temperature. Thus, at low pyrolysis temperatures there is hardly any influence of steam on the yields and composition of the product stream, as was confirmed in a previous study wherein the use of N_2 and steam as fluidizing agent was compared (Amutio et al., 2012; Fernandez et al., 2022). Therefore, steam has no significant effect on the product distribution obtained below 600 °C, i.e., the gas yield increases slightly from 19.5 wt% with N_2 to 22.9 wt% with steam, and bio-oil yield decreases from 65.1 wt% with N_2 to 62.1 wt% with steam. However, due to the endothermic nature of the reforming reactions (Ren et al., 2019), they are favored when pyrolysis temperature is increased and become significant above 700 °C. Thus, in view of the higher bio-oil yield and the composition of the gaseous fraction, steam has still little effect at 700 °C (due to the low residence time of the volatiles in the CSBR (Fernandez et al., 2022)), whereas gasification conditions are attained at 800 °C (reforming reactions are significant), leading to a considerable increase in the yield of the gas fraction.

Moreover, heterogeneous steam gasification of the char is promoted as temperature is increased, which has a significant effect on the overall pyrolysis-reforming process. On the one hand, a decrease in char yield involves an increase in the carbon content of the volatiles fed into the reforming reactor, increasing the potential for carbon conversion and consequently the potential for H_2 production. On the other hand, bearing in mind the possible application of the char as active carbon, a rise in temperature to around 800 °C increases char microporosity (char surface area increases from 16.2 m^2 g^{-1} to 495 m^2 g^{-1} when pyrolysis temperature raises from 500 to 800 °C, respectively), improving char surface properties and obtaining a solid product with commercial application (Fernandez et al., 2022; Alvarez et al., 2019b).

Regarding the individual yields of bio-oil compounds (Table 3), the main compounds obtained at low temperatures are phenols, whereas

Table 2

Effect of pyrolysis temperature on the product fractions yields (wt%) (95% confidence interval).

	500 °C	600 °C	700 °C	800 °C
Gas	**7.30 ± 0.29**	**22.88 ± 0.80**	**41.18 ± 1.61**	**63.92 ± 2.23**
CO	2.25	8.87	19.71	31.03
CO_2	4.68	11.67	15.08	21.94
CH_4	0.19	1.06	2.51	4.43
Light HCs (C_2-C_4)	0.12	0.96	3.01	4.62
H_2	0.06	0.32	0.87	1.9
Bio-oil	**75.36 ± 2.83**	**62.13 ± 2.55**	**46.32 ± 1.76**	**27.22 ± 1.06**
Char	**17.34 ± 0.81**	**15.00 ± 0.81**	**12.50 ± 0.81**	**8.86 ± 0.81**

Table 3
Effect of pyrolysis temperature on the yields of the individual bio-oil compounds (wt%).

	500 °C	600 °C	700 °C	800 °C
Acids	3.02	4.35	0.00	0.00
Aldehydes	2.48	5.70	7.72	0.26
Ketones	7.26	5.23	2.69	0.22
Alcohols	1.83	1.77	0.35	0.28
Polycyclic aromatic alcohols	0.21	0.00	0.51	0.62
Phenols	16.56	11.28	12.51	5.06
Alkyl-phenols	1.62	2.05	6.82	5.06
Catechols	8.28	8.67	5.69	0.00
Guaiacols	6.66	0.56	0.00	0.00
Furans	2.33	1.18	1.72	1.13
Saccharides	4.54	3.06	1.48	0.00
Hydrocarbons	0.00	0.47	0.99	8.76
BTX and light HCs	0.00	0.47	0.99	0.97
PAHs	0.00	0.00	0.00	7.79
Others	0.07	0.00	0.48	0.02
Unidentified	12.61	10.25	1.74	1.29
Water	24.45	18.84	16.13	9.57
Bio-oil	75.36	62.13	46.32	27.22

hydrocarbons are the prevailing ones at 800 °C. It is to note that the distribution of phenolic compounds changes with temperature, i.e., guaiacols and catechols are the main phenolic compounds at low temperatures, but they are destroyed to form more stable compounds at high temperatures, and so contribute to increasing the yield of alkyl-phenols and non-oxygenated hydrocarbons. This transformation of primary branched oxygenated compounds into tertiary aromatic compounds as temperature is increased is a general trend observed in literature for tar evolution (Font Palma, 2013; Hernández et al., 2013). Likewise, the yields of ketones, alcohols, furans and saccharides decrease as temperature is increased, since they are mainly formed by compounds with low thermal stability, such as levoglucosan (Shen et al., 2015).

The trend observed for acids and aldehydes is noteworthy, since their yields peak at the intermediate temperatures analyzed in this study, i.e., 600 and 700 °C, respectively. Thus, the yield of acids increases when temperature is raised from 500 to 600 °C due to the enhancement of acetic acid formation via deacetylation reactions (Kantarelis et al., 2013). Similarly, the yield of aldehydes peaks at 700 °C, presumably due to the formation of benzaldehyde-derived compounds from guaicol ones (Valderrama Rios et al., 2018). Nevertheless, the yield of both fractions is negligible at 800 °C due to their decomposition to yield more stable compounds, such as aromatic hydrocarbons and light hydrocarbons in the gaseous fraction.

Moreover, the yield of water is reduced as temperature is increased, revealing the aforementioned different role of steam depending on temperature, i.e., a higher amount of water reacts when temperature is raised due to the enhancement of steam reforming reactions at high temperatures. In fact, several steam pyrolysis studies conducted at low temperatures (500–600 °C) prove the negligible effect of steam on these reactions (Arregi et al., 2016; Fernandez et al., 2022), whereas biomass gasification studies show that a greater amount of steam reacts as temperature is increased (Cortazar et al., 2018; Erkiaga et al., 2014).

3.2. Effect of pyrolysis temperature on the activity and stability of the reforming catalyst

Once the influence of pyrolysis temperature on the composition of the volatiles was ascertained, the impact of the latter on the reforming catalyst activity and stability was analyzed. Thus, Fig. 2 shows the evolution of volatile conversion with time on stream and Fig. 3 the yields of the individual products. The following reactions have been considered for the evaluation of the results obtained:
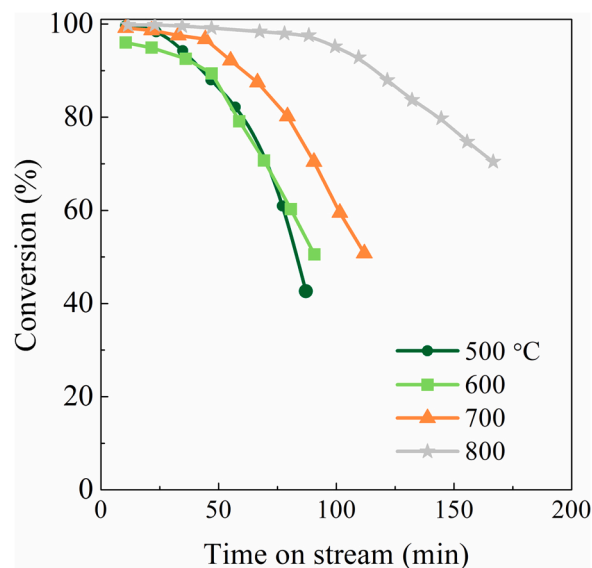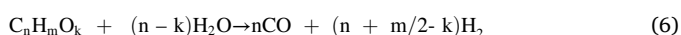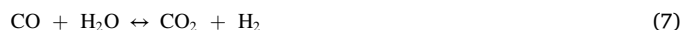
Steam reforming of oxygenates:

$$C_nH_mO_k + (n-k)H_2O \rightarrow nCO + (n + m/2- k)H_2 \quad (6)$$

Fig. 2. Effect of pyrolysis temperature on the conversion in the reforming of pyrolysis volatiles.

Water Gas Shift (WGS):

$$CO + H_2O \leftrightarrow CO_2 + H_2 \quad (7)$$

Cracking of oxygenates (secondary reaction):

$$C_nH_mO_k \rightarrow oxygenates + hydrocarbons + CH_4 + CO + CO_2 + C \quad (8)$$

Steam reforming of methane (and hydrocarbons):

$$CH_4 + H_2O \leftrightarrow CO + 3H_2 \quad (9)$$

Fig. 2 shows that initial conversion is almost full in the reforming of the biomass pyrolysis volatiles obtained at 500, 700 and 800 °C, as similar conversion values of 99.62%, 99.16% and 99.81%, respectively, are attained. However, when pyrolysis is carried out at 600 °C, a lower initial conversion is attained (96.01%). This poorer initial performance of the catalyst for the reforming of the volatiles obtained at 600 °C is related to the different composition of the volatile stream, especially to the higher yield of carboxylic acids and benzaldehydes contained in the fractions of acids and aldehydes, respectively (Table 3). In fact, the low reactivity of these compounds, mainly acetic acid, is well-known in the literature on the steam reforming of bio-oil (Remón et al., 2015; Bimbela et al., 2012; Cheng and Steam, 2017), with carboxylic acids being more refractory as their aliphatic carbon chain is longer (Li et al., 2018).

Regarding catalyst stability, significant differences were observed when biomass pyrolysis was performed at different temperatures. Thus, high influence of pyrolysis volatile composition on the catalyst performance and its deactivation is evidenced. An increase in pyrolysis temperature remarkably attenuates catalyst deactivation in the reforming step, achieving the best performance at a pyrolysis temperature of 800 °C. It must be noted that, under these conditions, the volatiles are partially gasified in the first reactor, with the yield of gaseous products being rather high (63.92 wt%) and that of bio-oil relatively low (27.22 wt%). The lower bio-oil yield to be reformed enhances the stability of the reforming catalyst. Furthermore, the composition of the bio-oil contributes to attenuating catalyst deactivation, since the concentration of oxygenated compounds decreases as temperature is increased, especially that of phenolic compounds (catechol and guaiacols), which are well-known as the main coke precursors by several authors (Ochoa et al., 2020; Trane-Restrup and Jensen, 2015; Valle et al., 2019). In view of these results, pyrolysis temperatures higher than 800 °C are expected to hinder the deactivation of the reforming catalyst. However, higher
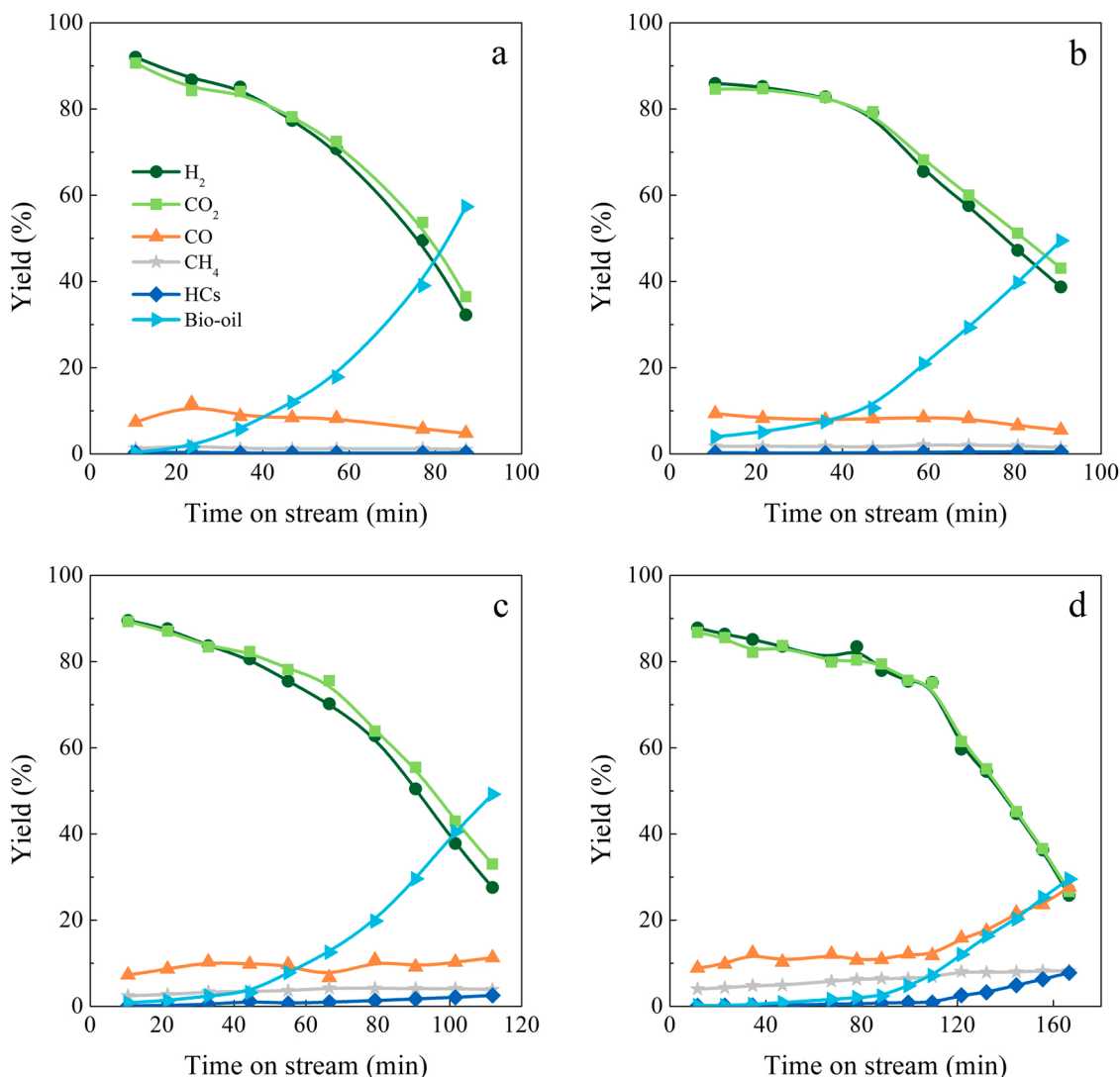
Fig. 3. Effect of pyrolysis temperature on the evolution of the individual product yields with time on stream in the reforming step. Pyrolysis temperatures: a) 500 °C; b) 600 °C; c) 700 °C; and d) 800 °C.

temperatures involve higher energy requirements and costs, which may not balance the higher stability of the reforming catalyst.

Although the initial conversion was the lowest when the biomass pyrolysis was performed at 600 °C, the deactivation rate was slightly lower than that observed in the reforming of the pyrolysis volatiles obtained at 500 °C, which decreased to 50.54% after 91 min on stream. This trend is related to the higher bio-oil yield obtained in the biomass pyrolysis carried out at 500 °C, i.e., a higher concentration of oxygenated compounds in the reaction environment, which leads to a faster catalyst deactivation (Arregi et al., 2017). Ochoa et al. (Ochoa et al., 2017) studied the role of oxygenated compounds in the coke formation and composition, identifying methoxyphenols (guaicols) and levoglucosan (saccharides) as the main coke precursors. Therefore, the different catalyst deactivation rate observed in the reforming of the volatiles obtained at 500 °C and 600 °C may be also related to the composition of the bio-oil obtained (Table 3). Thus, on the one hand, distribution of phenolic compounds changes, with a decrease of specially guaiacol yield when temperature is raised (6.66 wt% at 500 °C and 0.56 wt% at 600 °C) and, on the other hand, a lower yield of saccharides is obtained as temperature is raised (4.54 wt% at 500 °C and 3.06 wt% at 600 °C), with that of levoglucosan being especially lower.

Regarding the reforming of biomass pyrolysis volatiles obtained at 700 °C, an intermediate trend is observed, i.e., the commercial Ni/Al_2O_3

catalyst showed almost full conversion for the first 32 min on stream, but sharply decreased to 50.78% after 112 min on stream. This initial period of almost full conversion is longer than those observed at lower temperatures and must be related to the partial gasification attained in the first step, in which the yield of bio-oil was 46.32 wt% (Table 2). However, the deactivation of the reforming catalyst is relatively fast, which is presumably due to the composition of the pyrolysis volatiles obtained at 700 °C. In fact, this deactivation trend is attributed to the high yield of aldehydes (7.72 wt%), mainly benzaldehydes, and phenolic fraction (12.51 wt%), especially catechols, which are well-known as coke precursor compounds (Remón et al., 2015; Gayubo et al., 2005).

The results in Fig. 3 show the evolution of H_2, CO_2, CO, CH_4, C_2-C_4 hydrocarbons and non-converted bio-oil yields when different pyrolysis temperatures were used. As observed, the values obtained at initial times on stream are consistent with those shown in Fig. 2, with the lowest yield of H_2 (85.9%) and CO_2 (84.6%) attained in the reforming of the volatiles obtained at 600 °C. This is explained by the lower extension of reforming and WGS reactions due to the presence of more refractory compounds in the volatile stream, such as acetic acid (Remón et al., 2015; Cheng and Steam, 2017). Besides, although similar initial conversion values are obtained when the pyrolysis is carried out at 500 °C, 700 °C and 800 °C (Fig. 2), some differences are observed in the

individual yields of the products, such as the decrease in the initial yields of H_2 and CO_2 from 92.0% and 90.6% to 87.7% and 86.7%, respectively, when pyrolysis temperature is increased from 500 °C to 800 °C. Fig. 3 also shows that higher CH_4 yields are attained at the initial reaction stage as pyrolysis temperature is increased from 500 °C to 800 °C (from 1.3% to 4.0%), which is due to the higher CH_4 yield obtained in the pyrolysis step, i.e., higher CH_4 concentration in the volatile stream fed into the reforming reactor.

However, regarding the initial H_2 and gas productions obtained (Table 4), it can be observed that an increase in temperature has a positive effect on both values. It should be noted that these reaction indexes include not only the reforming step, but also the previous pyrolysis step, and they are defined per kg of biomass fed into the pyrolysis-reforming unit. Therefore, as pyrolysis temperature is increased from 500 °C to 800 °C, H_2 production increases from 9.56 wt% to 12.95 wt%, and the gas production from 1.71 Nm^3 kg^{-1} to 2.23 Nm^3 kg^{-1}. As aforementioned, this fact may be related to both the promotion of devolatilization and cracking of biomass compounds and the char gasification when pyrolysis temperature is increased (Table 2), as the char yield decreases from 17.34 wt% at 500 °C to 8.86 wt% at 800 °C, and therefore a higher amount of carbon is reformed in the second step. Consequently, the efficiency and carbon conversion of the pyrolysis-reforming process is favored as pyrolysis temperature is increased due to the enhancement of char gasification. Besides, the H_2 and gas production values obtained are higher than the ones previously obtained in the biomass pyrolysis-reforming on modified catalysts (Santamaria et al., 2020a, 2020b, 2020c), as well as in biomass gasification (Cortazar et al., 2021b). Furthermore, these values are significantly higher than those obtained by other authors in the literature (Santamaria et al., 2021; Islam, 2020).

Regarding the evolution of H_2 and CO_2 yields with time on stream, it can be seen that they decrease as time on stream is increased at any pyrolysis temperature due to the lower extent of steam reforming and WGS reactions when the reforming catalyst is deactivated. The effect of pyrolysis temperature on the evolution of H_2 and CO_2 yields is consistent with that observed for the evolution of volatile conversion (Fig. 2). Besides, Fig. 3 reveals that the non-converted bio-oil yield increases as reaction proceeds and the deactivation rate is higher due to the higher bio-oil concentration in the reaction environment, which is evidence of the role played by the non-converted bio-oil compounds as coke precursors. It should be noted that this autocatalytic deactivation behavior, i.e., faster catalyst deactivation when the concentration of coke precursors in the reaction medium is higher, was previously described in the steam reforming of biomass pyrolysis volatiles (Arregi et al., 2018b; Santamaria et al., 2020b, 2020c).

It is noteworthy that the trend in the evolution of CO yield depends on the pyrolysis temperature. Furthermore, catalyst deactivation has no significant effect on the CO yield in the reforming of the volatiles obtained at 500 °C and 600 °C due to the balance between the attenuation of reforming and WGS reactions and the enhancement of cracking reactions. However, an increase in CO yield is observed when biomass pyrolysis is carried out at 700 °C and especially at 800 °C, which is explained by the different pyrolysis volatile composition obtained, as CO concentration at the reactor inlet is higher at this temperature than at lower ones. Thereby, at the beginning of the reaction, the catalyst shows activity for WGS reaction and so CO/CO_2 ratio decreases, whereas this ratio increases, attaining values close to the reactor inlet composition,

when the catalyst is deactivated.

3.3. Coke deposition

The loss of activity in the Ni/Al$_2$O$_3$ reforming catalyst during pyrolysis and in-line steam reforming process is mainly caused by coke deposition. In fact, previous studies concluded that metal sintering is negligible at temperatures lower than Ni Tamman temperature (590 °C) (Santamaria et al., 2019, 2020b). Besides, it is known that the amount, nature and location of the coke deposited on the catalyst is related to the composition of the stream to be reformed (Ochoa et al., 2020). Thus, in order to evaluate the influence of the volatile composition obtained at different pyrolysis temperatures on the coke deposited, the deactivated catalysts were characterized by TPO and TEM. The derivative mass loss (DTG) profiles of the spent catalysts, i.e., TPO profiles, are shown in Fig. 4. Moreover, the results derived from the TPO profiles (coke amount and average coke deposition rate per biomass mass unit) are set out in Table 5.

As observed, the coke deposition rate on the catalysts decreases as pyrolysis temperature is raised, which is due to the lower bio-oil yield obtained in the pyrolysis step at high temperatures. Therefore, the highest coke deposition rate on the Ni/Al$_2$O$_3$ reforming catalyst (0.41 mg$_{coke}$ g$_{cat}^{-1}$ g$_{biomass}^{-1}$) occurs when pyrolysis has been carried out at 500 °C, which is consistent with the faster decrease in conversion (Fig. 2) and H_2 and CO_2 yields (Fig. 3) with time on stream. Hence, this highest coke deposition rate is related to the highest amount of bio-oil fed into the reforming step, as well as the composition of this bio-oil, i.e., high yields of phenolic compounds, especially catechols (8.28 wt%) and guaiacols (6.66 wt%), are obtained at 500 °C, with these phenolic compounds being identified as the main coke precursors by several authors (Trane-Restrup and Jensen, 2015; Valle et al., 2019; Ochoa et al., 2017).

The TPO profiles of the coke deposited on the catalyst (Fig. 4) clearly show that the composition of the pyrolysis volatiles affects not only to the amount of the coke deposited, but also its nature and location. According to the nature or morphology of the coke, three types are identified in the literature (Ochoa et al., 2020): i) encapsulating coke (combustion temperature below 500 °C) deposited on metal particles, which is generally formed from all types of hydrocarbons (oxygenated and non-oxygenated ones) adsorbed on the metal sites and subsequently condensed or polymerized; ii) filamentous coke (combustion
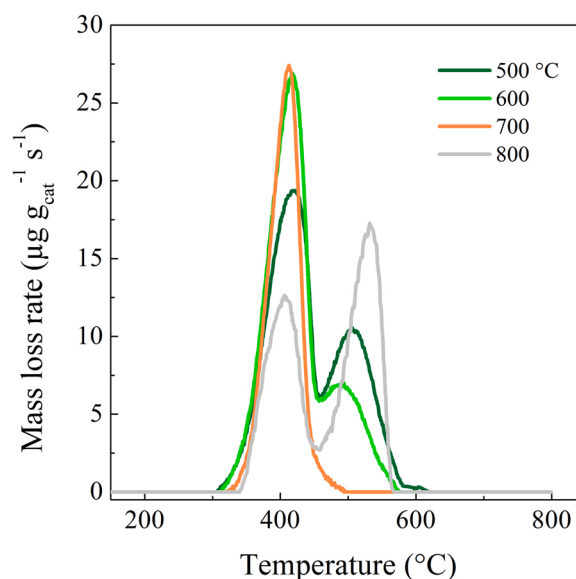

Fig. 4. Derivative mass loss rate (DTG) profiles of the catalyst deactivated at different pyrolysis temperatures.

Table 4

H$_2$ and gas productions obtained on the reforming catalysts at different pyrolysis temperatures. Reforming conditions: 600 °C; S/B ratio, 4; space time of 15 g$_{cat}$ min g$_{volatiles}^{-1}$.

	500 °C	600 °C	700 °C	800 °C
H$_2$ prod. (wt%)	9.56	9.93	10.78	12.95
Gas prod. (Nm^3 kg^{-1})	1.71	1.77	1.92	2.23

Table 5

Values of coke content (C_C) and total amount of coke deposited per biomass mass unit (r_C) on the Ni/Al$_2$O$_3$ catalyst.

Pyrolysis temperature	C_c	r_c	Time on stream	Biomass feed
(°C)	(wt%)	(mg$_{coke}$ g$_{cat}^{-1}$ g$_{biomass}^{-1}$)	(min)	(g)
500	2.66	0.41	87.1	65.3
600	2.11	0.31	90.6	68.0
700	1.59	0.19	111.9	83.9
800	1.37	0.11	166.6	125.0

temperature above 450 °C), which is generally formed by Boudouard reaction or CO reduction and decomposition of CH$_4$ and light hydrocarbons; and iii) pyrolytic coke (combustion temperature above 600 °C), which is formed by thermal cracking of oxygenated and non-oxygenated hydrocarbons under severe deactivation conditions. Apart from the coke morphology, the position of the coke in the catalyst particle has a great influence on the combustion temperature because combustion is catalyzed by metal sites, and coke combustion temperature decreases when they are close to one another (Ochoa et al., 2020; Santamaria et al., 2020a).

Fig. 4 shows two clearly differenced peaks at 425 °C and 500 °C, which are attributed to the combustion of the coke deposited on the catalyst. Based on the composition of the volatiles obtained at 500 °C

(Table 2 and Table 3), the first peak is due to the coke formed by the adsorption and condensation of bio-oil oxygenates on Ni active sites, whereas the second peak is related to either a more condensed structures composed of highly ordered aromatics or an amorphous coke deposited on the support (Ochoa et al., 2018).

It should be noted that the second peak decreases when pyrolysis is carried out at higher temperatures (600 °C and 700 °C), and may be correlated with the lower catalyst deactivation rate due the lower bio-oil amount in the volatile stream and so the lower yield of coke precursors, such as guaiacol compounds. In fact, Zhang et al. (Zhang et al., 2020b) reported that guaiacol and furfural produced not only a substantial amount of coke, which is related to the difficulty for cracking benzene ring structures, but the coke deposited was also more graphite like,
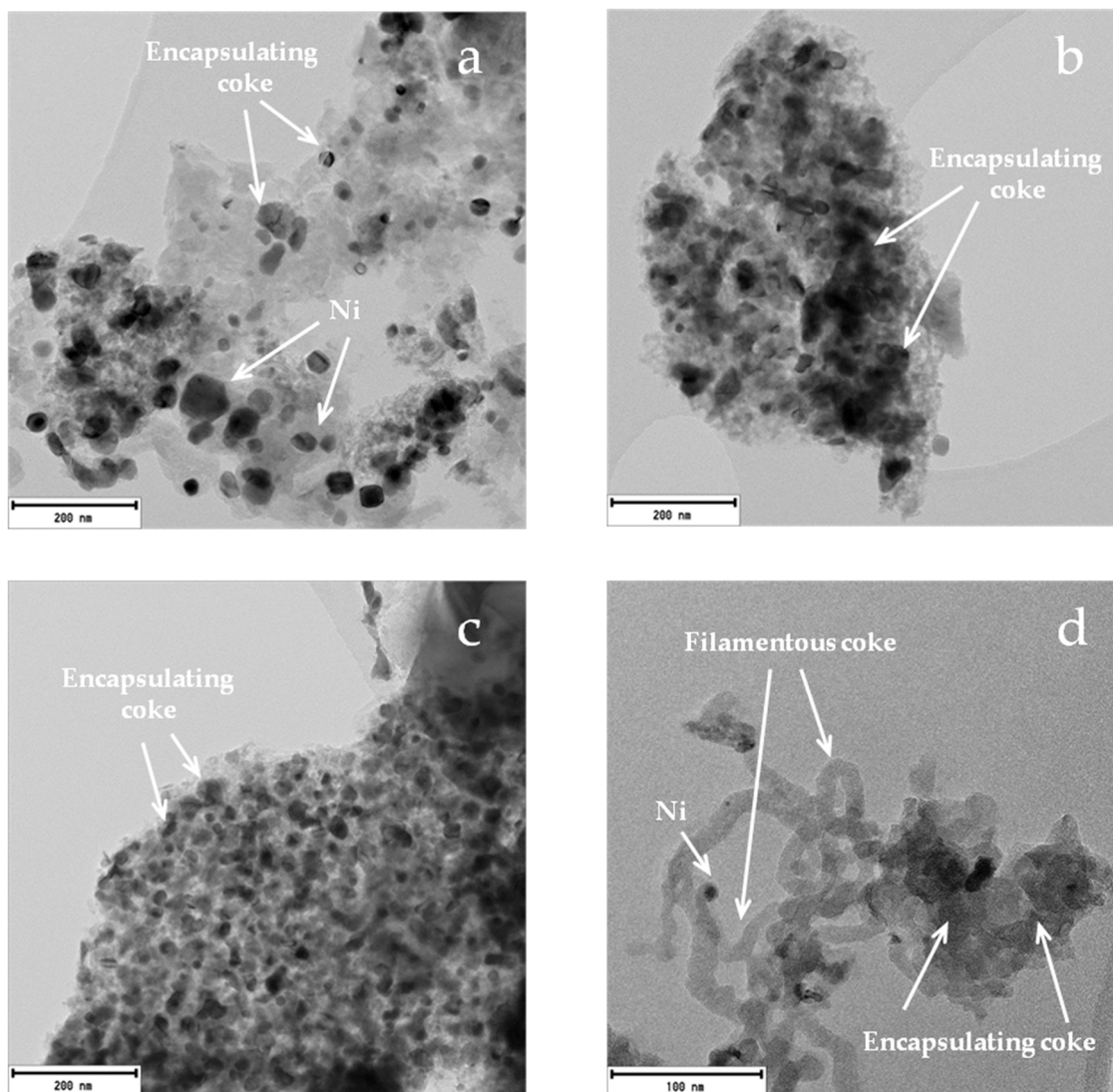

Fig. 5. TEM images of the deactivated catalyst. Pyrolysis temperatures: a) 500 °C; b) 600 °C; c) 700 °C; and d) 800 °C.

whose combustion temperature is higher. Moreover, previous results have demonstrated that, once the coke is deposited on the Ni sites (coke associated with the first combustion peak), its formation rate decreases, leading to the deposition of another type of coke on the support surface (that burning at around 500 °C) (Ochoa et al., 2018). Besides, the slight reduction in the first combustion peak in the run corresponding to a pyrolysis temperature of 500 °C is due to the higher evolution degree of coke precursors towards more condensed structures, i.e., more complex and of graphitic nature, as their yield is considerably higher than in the runs conducted at higher pyrolysis temperatures.

It is noteworthy that combustion peaks at higher temperatures (540 °C) are observed for the coke deposited on the catalyst in the reforming of the pyrolysis volatiles obtained at 800 °C. In this TPO profile, the first peak is associated with the encapsulating coke deposited on Ni active sites formed by oxygenated and non-oxygenated compounds in the reaction environment. However, the second peak is related to the filamentous coke, since the concentration of potential filamentous coke precursors (CO and CH_4) in the reaction environment is higher at this pyrolysis temperature than at lower ones (Table 2).

In order to gain insight into the coke nature and morphology of the coke deposited on the catalyst, Fig. 5 shows the TEM images of the catalyst used for reforming the streams obtained at the four pyrolysis temperatures. As observed, Ni^0 particles are identified as round shaped darkest regions in the image. It can be observed that the coke deposited on the catalyst used for reforming the pyrolysis volatiles obtained at 500, 600 and 700 °C is rather loose, with a disorder structure, and mainly deposited encapsulating the Ni particles. Regarding the TEM image of the coke deposited on the catalyst used in the reforming of the pyrolysis volatiles obtained at 800 °C, it can be seen that filamentous coke is also formed. This result is consistent with the TPO profiles (Fig. 4), and reveals that the higher amount of CO and light hydrocarbons in the pyrolysis volatiles obtained at 800 °C leads to the formation of filamentous carbon by Boudouard or decomposition reactions (Ochoa et al., 2020).

Once the main mechanisms of catalyst deactivation have been analyzed, further research on catalyst regeneration should be conducted in order to progress towards the scaling up of this pyrolysis-reforming process. In fact, a previous study was conducted in the same experimental unit in order to assess the regenerability of the commercial reforming catalyst used in this study (pyrolysis and reforming temperatures of 500 °C and 600 °C, respectively) (Arregi et al., 2018c). It was observed that, although the initial catalyst activity was not fully recovered due to the irreversible deactivation by metal sintering, a pseudo-stable state was reached beyond the fourth reaction-regeneration cycle.

4. Conclusions

Biomass pyrolysis (conducted in a CSBR at 500–800 °C) and the in-line steam reforming (in a fluidized bed reactor at 600 °C) perform well for H_2 production. Concerning the scaling up of the process, catalyst deactivation can be attenuated by modifying the temperature in the pyrolysis step, which allows tuning the composition of the volatiles to feed into the reforming step, and therefore lowering catalyst deactivation by coke deposition.

At low pyrolysis temperatures (500 °C), the product stream is mainly formed by bio-oil (75.36 wt%), in which phenols are the main fraction (16.56 wt%). However, an increase in temperature enhances devolatilization of biomass components and secondary cracking reactions leading to higher gas yields in detriment of the bio-oil one. Besides, the role of steam in the reaction mechanism has great influence on the volatiles obtained, as steam is inert at low temperatures, but takes part in gasification reactions at 800 °C. Thus, the gas fraction is the main one at 800 °C (63.92 wt%) and the bio-oil is mainly composed of PAH. Besides, devolatilization of biomass compounds and cracking reactions along with char steam gasification are favored, as its yield decreases

from 17.34 wt% at 500 °C to 8.86 wt% at 800 °C, and therefore, the overall carbon conversion in the process increases.

The reforming catalyst performance and stability is highly influenced by the volatile composition, with an increase in pyrolysis temperature attenuating the deactivation of the reforming catalyst. Thus, low pyrolysis temperatures lead to fast catalyst deactivation due to the large amount of bio-oil formed and its composition, which is mainly composed of potential coke precursors, such as phenols (guaiacols and catechol) and saccharides (levoglucosan). However, when pyrolysis step is carried out at 800 °C, catalyst deactivation is considerably attenuated and the catalyst maintains the initial activity for 67 min on stream. The enhancement of char gasification in the first step increases H_2 production (12.95 wt%), as well as gas production (2.23 Nm^3 kg^{-1}).

Deposition of coke on the catalyst surface is the main cause of the reforming catalyst deactivation, and its amount, nature and location in the catalyst are highly influenced by the composition of the pyrolysis volatiles. Thus, as pyrolysis temperature is increased, the average coke deposition rate decreases significantly (from 0.41 mg_{coke} $g_{cat}^{-1}g_{biomass}^{-1}$ at 500 °C to 0.11 mg_{coke} $g_{cat}^{-1}g_{biomass}^{-1}$ at 800 °C), which is consistent with the lower catalyst deactivation rate observed at higher temperatures. Therefore, the lower amount of bio-oil as well as the lower content of phenolic compounds in the volatile stream, attenuate catalyst deactivation by coke deposition. Besides, the nature of the coke is also affected by the volatile composition. Thus, encapsulating coke is formed by the adsorption and condensation of all hydrocarbons (oxygenated and non-oxygenated) on the Ni active sites at all pyrolysis temperatures, with coke amount being higher as the contents of bio-oil and phenolic fraction are higher. The volatile stream obtained at 800 °C leads to higher concentrations of CO and light hydrocarbons in the reaction environment, as well as filamentous carbon by Boudouard and decomposition reactions Santamaria 2020a, 2020c.

Declaration of Competing Interest

The authors declare that they have no known competing financial interests or personal relationships that could have appeared to influence the work reported in this paper.

References

Adeniyi, A.G., Otoikhian, K.S., Ighalo, J.O., 2019. Steam reforming of biomass pyrolysis oil: A review: Int. J. Chem. React. Eng. 17, 20180328. https://doi.org/10.1515/ijcre-2018-0328.

Ahmed, A., Al-Amin, A.Q., Ambrose, A.F., Saidur, R., 2016. Hydrogen fuel and transport system: A sustainable and environmental future. Int. J. Hydrog. Energy 41, 1369–1380. https://doi.org/10.1016/j.ijhydene.2015.11.084.

Akhtar, J., Saidina Amin, N., 2012. A review on operating parameters for optimum liquid oil yield in biomass pyrolysis. Renew. Sustain. Energy Rev. 16, 5101–5109. https://doi.org/10.1016/j.rser.2012.05.033.

Alvarez, J., Kumagai, S., Wu, C., Yoshioka, T., Bilbao, J., Olazar, M., Williams, P.T., 2014. Hydrogen production from biomass and plastic mixtures by pyrolysis-gasification. Int. J. Hydrog. Energy 39, 10883–10891. https://doi.org/10.1016/j.ijhydene.2014.04.189.

Alvarez, J., Lopez, G., Amutio, M., Mkhize, N.M., Danon, B., van der Gryp, P., Görgens, J. F., Bilbao, J., Olazar, M., 2017. Evaluation of the properties of tyre pyrolysis oils obtained in a conical spouted bed reactor. Energy 128, 463–474. https://doi.org/10.1016/j.energy.2017.03.163.

Alvarez, J., Amutio, M., Lopez, G., Santamaria, L., Bilbao, J., Olazar, M., 2019a. Improving bio-oil properties through the fast co-pyrolysis of lignocellulosic biomass

and waste tyres. Waste Manag. 85, 385–395. https://doi.org/10.1016/j.wasman.2019.01.003.

Alvarez, J., Lopez, G., Amutio, M., Bilbao, J., Olazar, M., 2019b. Evolution of biomass char features and their role in the reactivity during steam gasification in a conical spouted bed reactor. Energy Convers. Manag. 181, 214–222. https://doi.org/10.1016/j.enconman.2018.12.008.

Amutio, M., Lopez, G., Artetxe, M., Elordi, G., Olazar, M., Bilbao, J., 2012. Influence of temperature on biomass pyrolysis in a conical spouted bed reactor. Resour. Conserv. Recycl 59, 23–31. https://doi.org/10.1016/j.resconrec.2011.04.002.

Amutio, M., Lopez, G., Alvarez, J., Moreira, R., Duarte, G., Nunes, J., Olazar, M., Bilbao, J., 2013. Flash pyrolysis of forestry residues from the Portuguese Central Inland Region within the framework of the BioREFINA-Ter project. Bioresour. Technol. 129, 512–518. https://doi.org/10.1016/j.biortech.2012.11.114.

Amutio, M., Lopez, G., Alvarez, J., Olazar, M., Bilbao, J., 2015. Fast pyrolysis of eucalyptus waste in a conical spouted bed reactor. Bioresour. Technol. 194, 225–232. https://doi.org/10.1016/j.biortech.2015.07.030.

Arregi, A., Lopez, G., Amutio, M., Barbarias, I., Bilbao, J., Olazar, M., 2016. Hydrogen production from biomass by continuous fast pyrolysis and in-line steam reforming. RSC Adv. 6, 25975–25985. https://doi.org/10.1039/c6ra01657j.

Arregi, A., Amutio, M., Lopez, G., Artetxe, M., Alvarez, J., Bilbao, J., Olazar, M., 2017. Hydrogen-rich gas production by continuous pyrolysis and in-line catalytic reforming of pine wood waste and HDPE mixtures. Energy Convers. Manag. 136, 192–201. https://doi.org/10.1016/j.enconman.2017.01.008.

Arregi, A., Amutio, M., Lopez, G., Bilbao, J., Olazar, M., 2018a. Evaluation of thermochemical routes for hydrogen production from biomass: A review. Energy Convers. Manag. 165, 696–719. https://doi.org/10.1016/j.enconman.2018.03.089.

Arregi, A., Lopez, G., Amutio, M., Artetxe, M., Barbarias, I., Bilbao, J., Olazar, M., 2018b. Role of operating conditions in the catalyst deactivation in the in-line steam reforming of volatiles from biomass fast pyrolysis. Fuel 216, 233–244. https://doi.org/10.1016/j.fuel.2017.12.002.

Arregi, A., Lopez, G., Amutio, M., Barbarias, I., Santamaria, L., Bilbao, J., Olazar, M., 2018c. Regenerability of a Ni catalyst in the catalytic steam reforming of biomass pyrolysis volatiles. J. Ind. Eng. Chem. 68, 69–78. https://doi.org/10.1016/j.jiec.2018.07.030.

Artetxe, M., Lopez, G., Amutio, M., Barbarias, I., Arregi, A., Aguado, R., Bilbao, J., Olazar, M., 2015. Styrene recovery from polystyrene by flash pyrolysis in a conical spouted bed reactor. Waste Manag. 45, 126–133. https://doi.org/10.1016/j.wasman.2015.05.034.

Ashok, J., Kawi, S., 2021. Low-temperature biomass tar model reforming over perovskite materials with DBD plasma: Role of surface oxygen mobility. Energy Convers. Manag. 248, 114802 https://doi.org/10.1016/j.enconman.2021.114802.

Bimbela, F., Chen, D., Ruiz, J., García, L., Arauzo, J., 2012. Ni/Al coprecipitated catalysts modified with magnesium and copper for the catalytic steam reforming of model compounds from biomass pyrolysis liquids. Appl. Catal., B. 119–120, 1–12. https://doi.org/10.1016/j.apcatb.2012.02.007.

Cao, L., Yu, I.K.M., Xiong, X., Tsang, D.C.W., Zhang, S., Clark, J.H., Hu, C., Ng, Y.H., Shang, J., Ok, Y.S., 2020. Biorenewable hydrogen production through biomass gasification: A review and future prospects. Environ. Res. 186, 109547 https://doi.org/10.1016/j.envres.2020.109547.

Chen, J., Sun, J., Wang, Y., 2017. Catalysts for steam reforming of bio-oil: A review. Ind. Eng. Chem. Res. 56, 4627–4637. https://doi.org/10.1021/acs.iecr.7b00600.

Cheng, F., Steam, V.Dupont, 2017. reforming of bio-compounds with auto-reduced nickel catalyst. Catalysts 7, 114. https://doi.org/10.3390/catal7040114.

Cortazar, M., Alvarez, J., Lopez, G., Amutio, M., Santamaria, L., Bilbao, J., Olazar, M., 2018. Role of temperature on gasification performance and tar composition in a fountain enhanced conical spouted bed reactor. Energy Convers. Manag. 171, 1589–1597. https://doi.org/10.1016/j.enconman.2018.06.071.

Cortazar, M., Sun, S., Wu, C., Santamaria, L., Olazar, L., Fernandez, E., Artetxe, M., Lopez, G., Olazar, M., 2021a. Sorption enhanced ethanol steam reforming on a bifunctional Ni/CaO catalyst for H₂ production. J. Environ. Chem. Eng. 9, 106725 https://doi.org/10.1016/j.jece.2021.106725.

Cortazar, M., Santamaria, L., Lopez, G., Alvarez, J., Amutio, M., Bilbao, J., Olazar, M., 2021b. Fe/olivine as primary catalyst in the biomass steam gasification in a fountain confined spouted bed reactor. J. Ind. Eng. Chem. 99, 364–379. https://doi.org/10.1016/j.jiec.2021.04.046.

Di Stasi, C., Cortese, M., Greco, G., Renda, S., González, B., Palma, V., Manyà, J.J., 2021. Optimization of the operating conditions for steam reforming of slow pyrolysis oil over an activated biochar-supported Ni–Co catalyst. Int. J. Hydrog. Energy 46, 26915–26929. https://doi.org/10.1016/j.ijhydene.2021.05.193.

Dou, B., Zhang, H., Song, Y., Zhao, L., Jiang, B., He, M., Ruan, C., Chen, H., Xu, Y., 2019. Hydrogen production from the thermochemical conversion of biomass: issues and challenges. Sustain. Energy Fuels 3, 314–342. https://doi.org/10.1039/C8SE00535D.

Erkiaga, A., Lopez, G., Amutio, M., Bilbao, J., Olazar, M., 2014. Influence of operating conditions on the steam gasification of biomass in a conical spouted bed reactor. Chem. Eng. J. 237, 259–267. https://doi.org/10.1016/j.cej.2013.10.018.

Erkiaga, A., Lopez, G., Barbarias, I., Artetxe, M., Amutio, M., Bilbao, J., Olazar, M., 2015. HDPE pyrolysis-steam reforming in a tandem spouted bed-fixed bed reactor for H₂ production. J. Anal. Appl. Pyrolysis 116, 34–41. https://doi.org/10.1016/j.jaap.2015.10.010.

Fernandez, E., Santamaria, L., Artetxe, M., Amutio, M., Arregi, A., Lopez, G., Bilbao, J., Olazar, M., 2021a. In line upgrading of biomass fast pyrolysis products using low-cost catalysts. Fuel 296, 120682. https://doi.org/10.1016/j.fuel.2021.120682.

Fernandez, E., Amutio, M., Artetxe, M., Arregi, A., Santamaria, L., Lopez, G., Bilbao, J., Olazar, M., 2021b. Assessment of product yields and catalyst deactivation in fixed and fluidized bed reactors in the steam reforming of biomass pyrolysis volatiles.

Process Saf. Environ. Prot. 145, 52–62. https://doi.org/10.1016/j.psep.2020.07.039.

Fernandez, E., Santamaria, L., Amutio, M., Artetxe, M., Arregi, A., Lopez, G., Bilbao, J., Olazar, M., 2022. Role of temperature in the biomass steam pyrolysis in a conical spouted bed reactor. Energy 238, 122053. https://doi.org/10.1016/j.energy.2021.122053.

Font Palma, C., 2013. Modelling of tar formation and evolution for biomass gasification: A review. Appl. Energy 111, 129–141. https://doi.org/10.1016/j.apenergy.2013.04.082.

Gao, N., Salisu, J., Quan, C., Williams, P., 2021. Modified nickel-based catalysts for improved steam reforming of biomass tar: A critical review. Renew. Sustain. Energy Rev. 145, 111023 https://doi.org/10.1016/j.rser.2021.111023.

García-Gómez, N., Valle, B., Valecillos, J., Remiro, A., Bilbao, J., Gayubo, A.G., 2021. Feasibility of online pre-reforming step with dolomite for improving Ni spinel catalyst stability in the steam reforming of raw bio-oil. Fuel Process. Technol. 215, 106769 https://doi.org/10.1016/j.fuproc.2021.106769.

Gayubo, A.G., Aguayo, A.T., Atutxa, A., Valle, B., Bilbao, J., 2005. Undesired components in the transformation of biomass pyrolysis oil into hydrocarbons on an HZSM-5 zeolite catalyst. J. Chem. Technol. Biotechnol. 80, 1244–1251. https://doi.org/10.1002/jctb.1316.

González-Gil, R., Chamorro-Burgos, I., Herrera, C., Larrubia, M.A., Laborde, M., Mariño, F., Alemany, L.J., 2015. Production of hydrogen by catalytic steam reforming of oxygenated model compounds on Ni-modified supported catalysts. Simulation and experimental study. Int. J. Hydrog. Energy 40, 11217–11227. https://doi.org/10.1016/j.ijhydene.2015.05.167.

Hayashi, J.I., Hosokai, S., Sonoyama, N., 2006. Gasification of low-rank solid fuels with thermochemical energy recuperation for hydrogen production and power generation. Process Saf. Environ. Prot. 84, 409–419. https://doi.org/10.1205/psep06004.

Hernández, J.J., Ballesteros, R., Aranda, G., 2013. Characterisation of tars from biomass gasification: Effect of the operating conditions. Energy 50, 333–342. https://doi.org/10.1016/j.energy.2012.12.005.

Huang, J., Veksha, A., Chan, W.P., Lisak, G., 2021. Support effects on thermocatalytic pyrolysis-reforming of polyethylene over impregnated Ni catalysts. Appl. Catal., A 622, 118222. https://doi.org/10.1016/j.apcata.2021.118222.

Islam, M.W., 2020. A review of dolomite catalyst for biomass gasification tar removal. Fuel 267, 117095. https://doi.org/10.1016/j.fuel.2020.117095.

Kan, T., Strezov, V., Evans, T., He, J., Kumar, R., Lu, Q., 2020. Catalytic pyrolysis of lignocellulosic biomass: A review of variations in process factors and system structure. Renew. Sustain. Energy Rev. 134, 110305 https://doi.org/10.1016/j.rser.2020.110305.

Kantarelis, E., Yang, W., Blasiak, W., 2013. Production of liquid feedstock from biomass via steam pyrolysis in a fluidized bed reactor. Energy Fuels 27, 4748–4759. https://doi.org/10.1021/ef400580x.

Kumar, A., Chakraborty, J.P., Singh, R., 2017. Bio-oil: the future of hydrogen generation. Biofuels 8, 663–674. https://doi.org/10.1080/17597269.2016.1141276.

Kumar, R., Strezov, V., 2021. Thermochemical production of bio-oil: A review of downstream processing technologies for bio-oil upgrading, production of hydrogen and high value-added products. Renew. Sustain. Energy Rev. 135, 110152.

Lemonidou, A.A., Kechagiopoulos, P., Heracleous, E., Voutetakis, S., 2013a. - Steam reforming of bio-oils to hydrogen. In: Triantafyllidis, K.S., Lappas, A.A., Stöcker, M. (Eds.), The Role of Catalysis for the Sustainable Production of Bio-fuels and Bio-chemicals. Elsevier, Amsterdam, pp. 467–493.

Lemonidou, A.A., Vagia, E.C., Lercher, J.A., 2013b. Acetic Acid Reforming over Rh Supported on La₂O₃/CeO₂–ZrO₂: Catalytic Performance and Reaction Pathway Analysis. ACS Catal. 3, 1919–1928. https://doi.org/10.1021/cs4003063.

Li, D., Li, X., Gong, J., 2016. Catalytic reforming of oxygenates: State of the art and future prospects. Chem. Rev. 116, 11529–11653. https://doi.org/10.1021/acs.chemrev.6b00099.

Li, J., Jia, P., Hu, X., Dong, D., Gao, G., Geng, D., Xiang, J., Wang, Y., Hu, S., 2018. Steam reforming of carboxylic acids for hydrogen generation: Effects of aliphatic chain of the acids on their reaction behaviors. Mol. Catal. 450, 1–13. https://doi.org/10.1016/j.mcat.2018.02.027.

Li, X., Zhang, Z., Zhang, L., Fan, H., Li, X., Liu, Q., Wang, S., Hu, X., 2020. Investigation of coking behaviors of model compounds in bio-oil during steam reforming. Fuel 265, 116961. https://doi.org/10.1016/j.fuel.2019.116961.

Liu, Q., Xiong, Z., Syed-Hassan, S.S.A., Deng, Z., Zhao, X., Su, S., Xiang, J., Wang, Y., Hu, S., 2019. Effect of the pre-reforming by Fe/bio-char catalyst on a two-stage catalytic steam reforming of bio-oil. Fuel 239, 282–289. https://doi.org/10.1016/j.fuel.2018.11.029.

Lopez, G., Erkiaga, A., Artetxe, M., Amutio, M., Bilbao, J., Olazar, M., 2015. Hydrogen production by high density polyethylene steam gasification and in-line volatile reforming. Ind. Eng. Chem. Res. 54, 9536–9544. https://doi.org/10.1021/acs.iecr.5b02413.

Lopez, G., Santamaria, L., Lemonidou, A., Zhang, S., Wu, C., Sipra, A.T., Gao, N., 2022. Hydrogen generation from biomass by pyrolysis. Nat. Rev. Methods Prim. 2, 20. https://doi.org/10.1038/s43586-022-00097-8.

Martino, M., Ruocco, C., Meloni, E., Pullumbi, P., Palma, V., 2021. Main hydrogen production processes: An overview. Catalysts 11, 547. https://doi.org/10.3390/catal11050547.

Meloni, E., Martino, M., Iervolino, G., Ruocco, C., Renda, S., Festa, G., Palma, V., 2022. The Route from Green H₂ Production through Bioethanol Reforming to CO₂ Catalytic Conversion: A Review. Energies 15, 2383. https://doi.org/10.3390/en15072383.

Men, Y., Kolb, G., Zapf, R., Hessel, V., Löwe, H., 2007. Ethanol steam reforming in a microchannel reactor. Process Saf. Environ. Prot. 85, 413–418. https://doi.org/10.1205/psep07015.

Moulijn, J.A., van Diepen, A.E., Kapteijn, F., 2001. Catalyst deactivation: is it predictable?: What to do? Appl. Catal., A 212, 3–16. https://doi.org/10.1016/S0926-860X(00)00842-5.

Ochoa, A., Aramburu, B., Valle, B., Resasco, D.E., Bilbao, J., Gayubo, A.G., Castaño, P., 2017. Role of oxygenates and effect of operating conditions in the deactivation of a Ni supported catalyst during the steam reforming of bio-oil. Green. Chem. 19, 4315–4333. https://doi.org/10.1039/c7gc01432e.

Ochoa, A., Arregi, A., Amutio, M., Gayubo, A.G., Olazar, M., Bilbao, J., Castaño, P., 2018. Coking and sintering progress of a Ni supported catalyst in the steam reforming of biomass pyrolysis volatiles. Appl. Catal., B 233, 289–300. https://doi.org/10.1016/j.apcatb.2018.04.002.

Ochoa, A., Bilbao, J., Gayubo, A.G., Castaño, P., 2020. Coke formation and deactivation during catalytic reforming of biomass and waste pyrolysis products: A review. Renew. Sustain. Energy Rev. 119, 109600 https://doi.org/10.1016/j.rser.2019.109600.

Okolie, J.A., Epelle, E.I., Tabat, M.E., Orivri, U., Amenaghawon, A.N., Okoye, P.U., Gunes, B., 2022. Waste biomass valorization for the production of biofuels and value-added products: A comprehensive review of thermochemical, biological and integrated processes. Process Saf. Environ. Prot. 159, 323–344. https://doi.org/10.1016/j.psep.2021.12.049.

Palma, V., Ruocco, C., Meloni, E., Gallucci, F., Ricca, A., 2018a. Enhancing Pt-Ni/CeO$_2$ performances for ethanol reforming by catalyst supporting on high surface silica. Catal. Today 307, 175–188. https://doi.org/10.1016/j.cattod.2017.05.034.

Palma, V., Ruocco, C., Meloni, E., Ricca, A., 2018b. Oxidative reforming of ethanol over CeO$_2$-SiO$_2$ based catalysts in a fluidized bed reactor. Chem. Eng. Process. Process. Intensif. 124, 319–327. https://doi.org/10.1016/j.cep.2017.08.010.

Quan, C., Wang, H., Gao, N., 2020. Development of activated biochar supported Ni catalyst for enhancing toluene steam reforming. Int. J. Energy Res. 44, 5749–5764. https://doi.org/10.1002/er.5335.

Remiro, A., Valle, B., Aguayo, A.T., Bilbao, J., Gayubo, A.G., 2013. Steam reforming of raw bio-oil in a fluidized bed reactor with prior separation of pyrolytic lignin. Energy Fuels 27, 7549–7559. https://doi.org/10.1021/ef401835s.

Remón, J., Broust, F., Volle, G., García, L., Arauzo, J., 2015. Hydrogen production from pine and poplar bio-oils by catalytic steam reforming. Influence of the bio-oil composition on the process. Int. J. Hydrog. Energy 40, 5593–5608. https://doi.org/10.1016/j.ijhydene.2015.02.117.

Ren, J., Cao, J.P., Zhao, X.Y., Yang, F.L., Wei, X.Y., 2019. Recent advances in syngas production from biomass catalytic gasification: A critical review on reactors, catalysts, catalytic mechanisms and mathematical models. Renew. Sustain. Energy Rev. 116, 109426 https://doi.org/10.1016/j.rser.2019.109426.

Saldarriaga, J.F., Aguado, R., Pablos, A., Amutio, M., Olazar, M., Bilbao, J., 2015. Fast characterization of biomass fuels by thermogravimetric analysis (TGA. Fuel 140, 744–751. https://doi.org/10.1016/j.fuel.2014.10.024.

Santamaria, L., Lopez, G., Arregi, A., Amutio, M., Artetxe, M., Bilbao, J., Olazar, M., 2019. Stability of different Ni supported catalysts in the in-line steam reforming of biomass fast pyrolysis volatiles. Appl. Catal., B. 242, 109–120. https://doi.org/10.1016/j.apcatb.2018.09.081.

Santamaria, L., Lopez, G., Arregi, A., Amutio, M., Artetxe, M., Cortazar, M., Amutio, M., Bilbao, J., Olazar, M., 2020a. Effect of CeO$_2$ and MgO promoters on the performance of a Ni/Al$_2$O$_3$ catalyst in the steam reforming of biomass pyrolysis volatiles. Fuel Process. Technol. 198, 106223 https://doi.org/10.1016/j.fuproc.2019.106223.

Santamaria, L., Arregi, A., Lopez, G., Artetxe, M., Amutio, M., Bilbao, J., Olazar, M., 2020b. Effect of La$_2$O$_3$ promotion on a Ni/Al$_2$O$_3$ catalyst for H$_2$ production in the in-

line biomass pyrolysis-reforming. Fuel 262, 116593. https://doi.org/10.1016/j.fuel.2019.116593.

Santamaria, L., Lopez, G., Arregi, A., Artetxe, M., Amutio, M., Bilbao, J., Olazar, M., 2020c. Catalytic steam reforming of biomass fast pyrolysis volatiles over Ni–Co bimetallic catalysts. J. Ind. Eng. Chem. 91, 167–181. https://doi.org/10.1016/j.jiec.2020.07.050.

Santamaria, L., Lopez, G., Fernandez, E., Cortazar, M., Arregi, A., Olazar, M., Bilbao, J., 2021. Progress on catalyst development for the steam reforming of biomass and waste plastics pyrolysis volatiles: A review. Energy Fuels 35 (21), 17051–17084. https://doi.org/10.1021/acs.energyfuels.1c01666.

Setiabudi, H.D., Aziz, M.A.A., Abdullah, S., Teh, L.P., Jusoh, R., 2020. Hydrogen production from catalytic steam reforming of biomass pyrolysis oil or bio-oil derivatives: A review. Int. J. Hydrog. Energy 45, 18376–18397. https://doi.org/10.1016/j.ijhydene.2019.10.141.

Shen, D., Jin, W., Hu, J., Xiao, R., Luo, K., 2015. An overview on fast pyrolysis of the main constituents in lignocellulosic biomass to valued-added chemicals: Structures, pathways and interactions. Renew. Sustain. Energy Rev. 51, 761–774. https://doi.org/10.1016/j.rser.2015.06.054.

Tang, W., Cao, J., Wang, Z., He, Z., Liu, T., Wang, Z., Yang, F., Ren, J., Zhao, X., Feng, X., Bai, H., 2021. Comparative evaluation of tar steam reforming over graphitic carbon supported Ni and Co catalysts at low temperature. Energy Convers. Manag. 244, 114454 https://doi.org/10.1016/j.enconman.2021.114454.

Trane-Restrup, R., Jensen, A.D., 2015. Steam reforming of cyclic model compounds of bio-oil over Ni-based catalysts: Product distribution and carbon formation. Appl. Catal., B 165, 117–127. https://doi.org/10.1016/j.apcatb.2014.09.026.

Vagia, E.C., Lemonidou, A.A., 2010. Investigations on the properties of ceria–zirconia-supported Ni and Rh catalysts and their performance in acetic acid steam reforming. J. Catal. 269, 388–396. https://doi.org/10.1016/j.jcat.2009.11.024.

Valderrama Rios, M.L., González, A.M., Lora, E.E.S., Almazán del Olmo, O.A., 2018. Reduction of tar generated during biomass gasification: A review. Biomass-.-. Bioenergy 108, 345–370. https://doi.org/10.1016/j.biombioe.2017.12.002.

Valle, B., García-Gómez, N., Arandia, A., Remiro, A., Bilbao, J., Gayubo, A.G., 2019. Effect of phenols extraction on the behavior of Ni-spinel derived catalyst for raw bio-oil steam reforming. Int. J. Hydrog. Energy 44, 12593–12603. https://doi.org/10.1016/j.ijhydene.2018.12.057.

Wang, S., Mukhambet, Y., Esakkimuthu, S., Abomohra, A.E., 2022. Integrated microalgal biorefinery – Routes, energy, economic and environmental perspectives. J. Clean. Prod. 348, 131245 https://doi.org/10.1016/j.jclepro.2022.131245.

Zhang, L., Yu, Z., Li, J., Zhang, S., Hu, S., Xiang, J., Wang, Y., Liu, Q., Hu, G., Hu, X., 2020b. Steam reforming of typical small organics derived from bio-oil: Correlation of their reaction behaviors with molecular structures. Fuel 259, 116214. https://doi.org/10.1016/j.fuel.2019.116214.

Zhang, Z., Ou, Z., Qin, C., Ran, J., Wu, C., 2019. Roles of alkali/alkaline earth metals in steam reforming of biomass tar for hydrogen production over perovskite supported Ni catalysts. Fuel 257, 116032. https://doi.org/10.1016/j.fuel.2019.116032.

Zhang, Z., Zhang, X., Zhang, L., Wang, Y., Li, X., Zhang, S., Liu, Q., Wei, T., Gao, G., Hu, X., 2020a. Steam reforming of guaiacol over Ni/SiO$_2$ catalyst modified with basic oxides: Impacts of alkalinity on properties of coke. Energy Convers. Manag. 205, 112301 https://doi.org/10.1016/j.enconman.2019.112301.

Zhao, Z., Situmorang, Y.A., An, P., Chaihad, N., Wang, J., Hao, X., Xu, G., Abudula, A., Guan, G., 2020. Hydrogen production from catalytic steam reforming of bio-oils: A critical review. Chem. Eng. Technol. 43, 625–640. https://doi.org/10.1002/ceat.201900487.